RSC Advances

PAPER

View Article Online
View Journal | View Issue

Cite this: *RSC Adv.*, 2022, **12**, 8477

Development of new 2-piperidinium-4-styrylcoumarin derivatives with large Stokes shifts as potential fluorescent labels for biomolecules†

Raquel Eustáquio,[a] João P. Prates Ramalho,[bc] Ana T. Caldeira[ab] and António Pereira*[ab]

Received 2nd February 2022
Accepted 3rd March 2022

DOI: 10.1039/d2ra00716a

rsc.li/rsc-advances

A series of novel 2-piperidinium-4-styrylcoumarin derivatives, with large Stokes shifts and high fluorescence quantum yields, were synthesized using an efficient and low-cost synthetic strategy as potential fluorescent labels for biomolecules. Density functional theory and time-dependent density functional theory calculations were performed in order to rationalize the observed photophysical properties.

1 Introduction

Fluorescence microscopy is a highly sensitive imaging technique that allows for the detection, tracking and visualization of biomolecules in analytical studies in many important scientific areas such as medicine, pharmacy, cellular biology and environmental sciences, among others.[1–5] One of the great advantages of fluorescence microscopy is the possibility of using several fluorescent labels to detect different biomolecules and produce multicolour images that allow for the identification of specific components of complex biomolecular assemblies, *in vitro* and *in vivo*, as well the analysis of their interactions.[1,6–8] Moreover, fluorescent labelling, taking into account the extraordinary sensitivity of the fluorescence technique and its non-destructive nature, also exhibits numerous advantages such as the use of small sample quantities as well as specific fluorescent labels.[9] Fluorescent labels can produce chemically stable and small-in-size bioconjugates, with insignificant interference to the structure and biological functions of the unlabelled biomolecules.[10] Amine-reactive fluorescent labels, due to the abundance of amino groups or their easy insertion into biomolecules, are very frequently used to prepare bioconjugates for multiple biological applications such as histochemistry, cell tracing, receptor binding, fluorescence *in situ* hybridization (FISH) or direct and indirect immunochemistry.[11–14] However, for multicolour imaging experiments, efficient spectral separation of different labels into two or more excitation or detection channels is necessary and essential because cross-talk between the excitation and emission spectra often generates self-quenching and a poor signal-to-noise ratio.[1,15] Fluorescent labels with large Stokes shifts are thus indispensable in multicolour super-resolution techniques such as the optical microscopy of biomolecules based on stimulated emission depletion (STED).[1,15,16] These kinds of chromophores are also very important in Förster-type resonance energy transfer (FRET) applications.[16,17] In this context, the development of new fluorophores with large and adjustable Stokes shifts is of utmost importance as they allow for the reduction of the number of detection channels, avoiding cross-talk and contributing to accurate sensing and precise multicolour imaging.[1,15–19] Currently, the most widely used available fluorescent labels are very expensive and some display small Stokes shifts of less than 30 nm (*e.g.*, fluorescein, rhodamine, oxazine and cyanine), which is why coumarin derivatives can be a solution to develop low-cost new bright fluorophores, with large Stokes shifts.[15,20] Coumarins, in addition to their great significant biological activity,[21,22] constitute one of the main classes of fluorescent dyes used currently in many applications.[23–30] Advances in past years have demonstrated that the nature of the substituents and their substitution pattern in the coumarin rings clearly affect the delocalization of the conjugated π-electron system. Furthermore, it is well known that the presence of these substituents involving donor bridge acceptor structures (D–π–A) can create an efficient process of intramolecular charge transfer (ICT) and promote diversified and exceptional photophysical properties in the coumarin derivatives.[1,20,24,31–34] In this work, we intend to develop a low-cost and effective synthetic strategy to synthesize new red-shifted 2-piperidinium coumarin derivatives as potential fluorescent labels for biomolecules using inexpensive 7-diethylamino-4-methylcoumarin (**1**) as a starting material. The referred coumarin **1** with their electron-

[a]*HERCULES Laboratory, City University of Macau Chair in Sustainable Heritage, University of Évora, Largo Marquês de Marialva 8, 7000-809 Évora, Portugal. E-mail: amlp@uevora.pt*

[b]*Chemistry Department, School of Sciences and Technology, University of Évora, Rua Romão Ramalho 59, 7000-671 Évora, Portugal*

[c]*LAQV-REQUIMTE, University of Évora, Rua Romão Ramalho 59, 7000-671 Évora, Portugal*

† Electronic supplementary information (ESI) available: NMR and mass spectra and quantum chemical calculations. See DOI: 10.1039/d2ra00716a

donating group (EDG) at position 7 creates an evident push–pull effect with the electron-withdrawing lactone moiety, promoting greater bathochromic shifts in the absorption spectrum compared to other donating substituents, such as alkoxy groups.[33] To complement this study, a theoretical analysis on the optical, electronic and geometrical properties of the coumarin derivatives, in the ground and lowest-lying singlet-excited states, has been carried out by means of Density Functional Theory (DFT) and Time-Dependent Density Functional Theory (TD-DFT).

2 Results and discussion

2.1 Synthesis

The key molecule in the synthesis of these new red-shifted chromophores is the 2-piperidinium coumarin derivative **3**, which was easily obtained after the thionation reaction in the carbonyl group of the 7-diethylamino-4-methylcoumarin (**1**)[33] followed by condensation of such thionated coumarin (**2**) with piperidine (Scheme 1), in very good yield (85%). This very interesting new "green" molecule (Fig. 1), exhibits a higher bathochromic shift than 66 nm when compared with its precursor (**1**). Additionally, and with the aim of increasing the π delocalization and obviously the push–pull character of the molecule, we idealized the inclusion of one additional styryl group in position 4 in the referred 2-piperidinium coumarin derivative (**3**). The presence of electron-donating groups (EDGs) or electron-withdrawing groups (EWGs) at *para* position, in this case, the 4-styryl group can improve the photophysical properties of the respective derivatives, such as higher bathochromic and large Stokes shifts, as well as high fluorescence quantum yields. According to the aforementioned discussion, we describe the synthesis and spectroscopic characterization of a small library of 2-piperidinium-4-styrylcoumarin derivatives to explore the effect of EDGs and EWGs on the photophysical properties of the new chromophores. Additionally, considering the binomial photophysical properties and cost, one of the best candidates was functionalized as an effective fluorescent label for biomolecules through a reactive succinimidyl ester group. The main synthetic strategy for synthesizing the 2-piperidinium coumarin derivatives was outlined considering the possible aldol condensation reactions at position 4 due to the high acidity of the methyl protons present in 1-(7-(diethylamino)-4-methyl-2*H*-chromen-2-ylidene)piperidin-1-ium nitrate (**3**). The

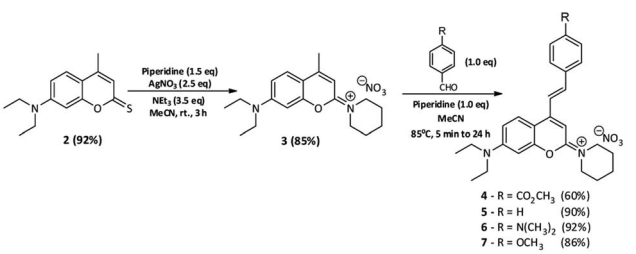

Scheme 1 Synthetic route of the 2-piperidinium-4-styrylcoumarin derivatives.

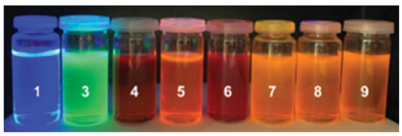

Fig. 1 Photographic images of the coumarin derivatives (**1**, **3**–**9**) in MeCN at 365 nm.

synthetic routes followed for the preparation of the novel 2-piperidinium coumarin derivatives (**4** to **7**) are shown in Scheme 1. 2-Piperidinium-4-styrylcoumarin derivatives (**4** to **7**) were obtained through highly efficient and stereoselective aldol condensation reactions between the aromatic aldehydes (methyl 4-formylbenzoate, benzaldehyde, 4-(dimethylamino) benzaldehyde and 4-methoxybenzaldehyde) and the 2-piperidinium coumarin derivative **3**, in good to high yields. The abovementioned new products (Fig. 1) were easily isolated after silica column chromatography and were fully characterized by NMR spectroscopy and HRMS (SI). All the spectral data are consistent with the proposed structures.

2.2 Photophysical properties

Photophysical properties of all synthesized coumarin derivatives were studied, and their absorption and emission properties, as well as fluorescence quantum yields, are summarised in Table 1. The absorption and emission spectra of the new 2-piperidinium-4-styrylcoumarin derivatives (**4** to **7**) are displayed in Fig. 2. Almost all 2-piperidinium-4-styrylcoumarin derivatives (**4** to **6**), exhibit absorption and emission maxima at longer wavelengths, when compared to intermediate, 2-piperidinium coumarin derivative **3**, possibly due to the intramolecular charge transfer effect between the coumarin electron-donating NEt_2 groups are conjugated with the styryl groups in position 4 and the electron-withdrawing piperidinium group in position 2. The derivatives **7**, **8** and **9**, with oxygen as an electron donor atom in the 4-styryl group, have different behaviour from other derivatives, with a hypsochromic shift in the absorption spectrum but with a bathochromic shift in the emission spectrum, which gives them large Stokes shifts (Table 1). In general, all the coumarin derivatives exhibit large Stokes shifts due to the extension of π – the conjugated system in the molecule, which is essential to an effective intramolecular charge transfer process of the emissive excited state. The possible elimination of the spectral overlap between absorption and emission, in fluorophores with large Stokes shifts, allows to eliminate the quenching process and reduce interference, providing effective detection of the fluorescence emission. Generally, the presence of electron-withdrawing groups at position 4 promotes higher bathochromic shifts than the electron-donating groups,[34] but this effect is not observed in the 2-piperidinium-4-styrylcoumarin derivatives (**4** to **7**), possibly due to the strong electron-withdrawing effect of the piperidinium-positive charge in position 2. On the other hand, the molar extinction coefficients were strongly affected by the nature of EDGs or EWGs in the *para* position at the 4-styryl group. The analysis shown in

Table 1 Spectroscopic properties of the 7-diethylamino-4-methyl-coumarin derivatives

Compound	λ_{abs}[a] (nm)	λ_{em}[b] (nm)	Stokes shift (nm, cm^{-1})	ε[c] (cm^{-1} M^{-1})	Φ_F[d]
1	371	434	63, 3913	22 910	0.73
3	437	490	53, 2475	21 000	0.14
4	484	609	125, 4241	18 000	0.08
5	467	525	58, 2366	17 000	0.34
6	485	608	123, 4171	39 000	0.98
7	410	578	168, 7089	30 000	0.82
8	406	578	172, 7330	30 000	0.90
9	404	577	173, 7421	30 000	0.92

[a] Absorption maxima in acetonitrile. [b] Emission maxima in acetonitrile. [c] Molar extinction coefficient at longest wavelength transition. [d] Fluorescence quantum yield in ethanol, determined at 25 °C using 7-diethylamino-4-methylcoumarin ($\Phi_F = 0.73$ in ethanol) as a standard.[33]

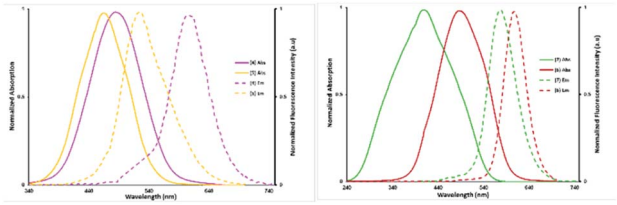

Fig. 2 Absorbance and emission spectra of the new 2-piperi-dinium-4-styrylcoumarin derivatives **4**, **5** (left) and **6**, **7** (right).

Table 1 allows to verify that in the case of the 2-piperidinium-4-styrylcoumarin derivatives (**4** to **7**), EDGs promote high coefficients [*e.g.*, ε (**6**) = 39 000 cm^{-1} M^{-1} *vs.* ε (**4**) = 18 000 cm^{-1} M^{-1}] and also high fluorescence quantum yields [*e.g.*, Φ_F (**6**) = 0.98 *vs.* Φ_F (**4**) = 0.08]. The extension of the π-conjugated system generally promotes an effective intramolecular charge transfer process that can cause the decrease of fluorescence quantum yield in the molecules.[35] This effect is not observed for compounds **6** and **7**, as they present high fluorescence quantum yields, possibly due to the presence of strong electron-donating substituents in the *para* position of the styryl groups.[36] Considering the large Stokes shift and the high fluorescence quantum yield induced by the methoxy group in the 2-piperidinium-4-styrylcoumarin derivative **7** (Table 1), we selected this electron-donating substituent to synthesize an effective and inexpensive fluorescent label for biomolecules. The aldol condensation of **3** with the 6-(4-formylphenoxy)hexanoic acid afforded the derivative **8**, which further reacted with *N*-hydroxysuccinimide to obtain the fluorescent label **9** (Scheme 2). The referred fluorescent label can be obtained through five linear and effective synthetic steps from inexpensive, commercially available precursors and as expected, its photophysical properties are very similar to those of derivative **7**.

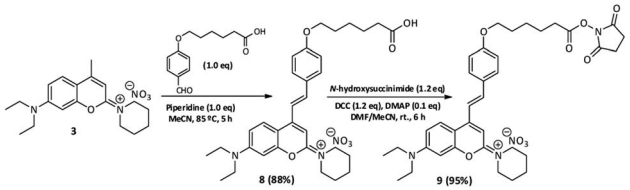

Scheme 2 Synthesis of an amine-reactive fluorescent label for biomolecules.

2.3 Theoretical calculations

The experimental and calculated absorption spectra together with the frontier orbitals involved in the lowest energy transitions of a selection of coumarin derivatives are depicted in Fig. 3. The general agreement between the calculated and the experimentally measured absorption spectra is quite good being able to capture its main features and to allow the assignment of the lowest energy absorption bands in terms of orbital transitions. For coumarin derivatives **4** and **5**, the S0 → S1 or S0 → S2 transitions are well separated, giving rise to the two absorption bands depicted in the experimental spectra. For other compounds, these transitions present closer energies and coalesce to a single band as observed in the experimental spectra. Whereas in LUMO the charge is largely delocalized throughout the molecule, in HOMO and HOMO-1 orbitals it is mainly localized either in the 4-styryl moiety or in the coumarin rings. However, while the HOMO state is mainly located on the coumarin moiety for compounds **4**, **5**, **7** and **9**, for compound **6** the HOMO state is mostly located in the 4-styryl group. The situation is the opposite for the HOMO-1 state, which is located on the 4-styryl group for compounds **4**, **5**, **7** and **9** while for compound **6** it is in the coumarin moiety. Comparing the absorption spectra and MOs of compounds **7** and **9** they are

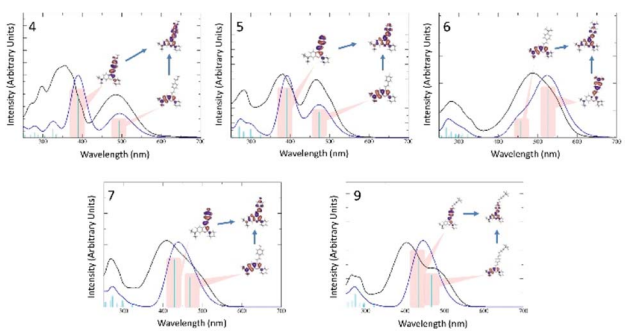

Fig. 3 Experimental spectra (black) compared with the calculated spectra (blue) and contour plots of the molecular orbitals involved in the two lowest energy excitations.

similar since the attached reactive group does not take part in the π-conjugation framework, thus justifying very similar photophysical properties. The maximum absorption wavelengths and the oscillator strength (*f*) of the key transitions were calculated and are depicted in Fig. 4 and Table S2,† together with the assigned main components of the transitions. A visual picture of electronic rearrangement that occurs upon the lowest (and most important) transitions is given by electronic density differences of the states involved in the transitions. The electron density difference of the lowest energy excitations is displayed in Fig. 4, illustrating the regions of the molecules that lose or gain electron charge. All compounds present two lowest-energy excitations S0 → S1 and S0 → S2 showing the final state, the LUMO, and as starting states the HOMO and HOMO-1 states, respectively. For all compounds, except compound **6**, S0 → S1 accounts for an electron density flow from the 4-styryl group towards the coumarin moiety, whereas S0 → S2 represents an electron density transfer to the 4-styryl group. For compound **6**, however, the electron flows occur in the opposite direction. However, for all compounds, the most probable transition, *i.e.*, that with the higher oscillator strength, despite being S0 → S1 or S0 → S2, corresponds to a decrease in electronic density in the 4-styryl pendant and a transfer of charge to the coumarin moiety. It is also for this compound that the higher oscillator strength corresponds to the lowest energy transition, thus dominating the absorption spectrum and indicating the intense donor capability of the amine group bond to the 4-styryl moiety. A central factor that affects the emission process is the structural changes that possibly occur on the geometry of the excited states after vertical excitation.[37,38] A large Stokes shift is expected if significant structural relaxation occurs in the excited state prior to emission. The optimized geometry of the studied coumarin derivatives in the electronic ground and first excited states are depicted in Fig. S2.† In the ground state, the compounds show a significant deviation from planarity with the plane of the 4-styryl group rotated relatively to the coumarin rings moiety plane. The torsion occurs on the bond that joins the coumarin ring moiety and the 4-styryl group, with the ethylene bridge being nearly in the plane with the pendant benzyl group (see ESI† for details). This dihedral angle presents values between 15° for compound **6** and 26° for compound **4** and limits the π conjugation system that links the donor and acceptor groups in the molecules.

On the excited S1 state, however, after the structural relaxation, the dihedral angle changes to a minimum of 2° for compound **4** and a maximum of 7° for compound **6**, therefore, the molecules become more planar. Also, the calculated bond length alternation (BLA, the average difference between a single and adjacent double bond length) for the small 4-styryl conjugated chain, attains 0.11 A for compounds **4** and **5**, 0.10 A for compounds **7** and **9** and 0.08 A for compound **6**, in the S0 state. For the S1 state, the BLA reduces to 0.06 A for compound **6** and 0.04 A for all other compounds. These changes in geometry contribute to an enhancement of the electronic delocalization throughout the π-conjugation framework and a decrease in the HOMO and LUMO energy gap, thus resulting in smaller emission energy compared with the excitation energy.

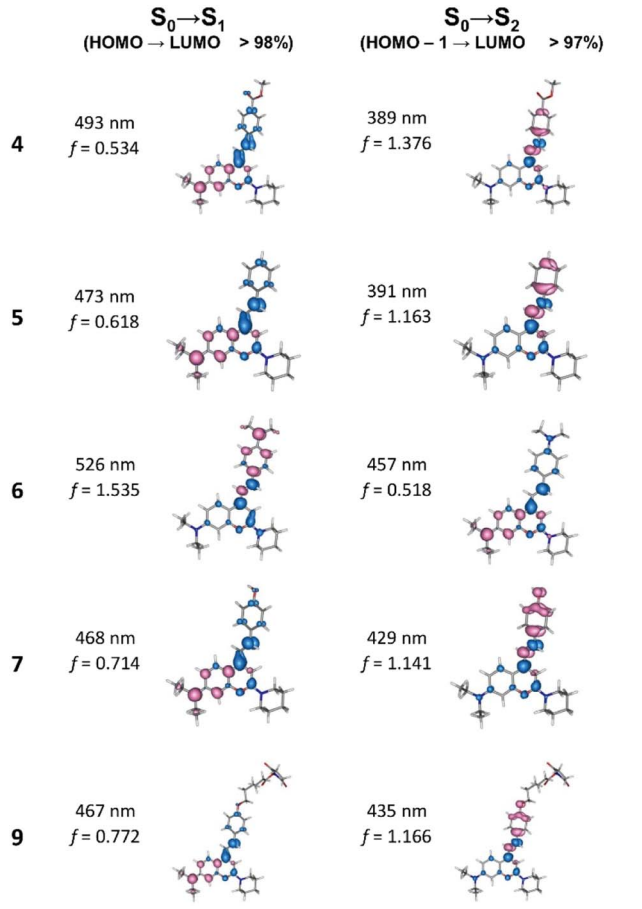

Fig. 4 Contour plots of the electron density difference $\Delta\rho(r)$ upon the lowest energy excitations for the studied compounds. Blue colour indicates an increase of electron density upon the transition, while pink represents a depletion of electron density.

3 Materials and methods

3.1 General methods

All starting materials and reagents were of analytical grade, purchased from Aldrich and used without further purification. The organic solvents were dried over appropriate drying agents and distilled prior to use. UV-Vis absorption spectra were recorded on the Nicolet Evolution 300, Thermo Electron Spectrophotometer Corporation, using acetonitrile (CH_3CN) as a solvent. Fluorescence measurements of aerated solutions were performed on a PerkinElmer Model LS 55 spectrofluorometer. All emission spectra were collected at 5.0 nm slit bandwidth for excitation and emission, with correction files. All spectroscopic measurements were performed in 3 mL quartz fluorescence cuvettes (1 cm optical path) at 21 °C. FTMS-ESI mass spectra were obtained on a Thermo Scientific Q Exactive Orbitrap Mass Spectrometer. Nuclear magnetic resonance (NMR) spectra were recorded at 400 MHz for ^{1}H NMR and 100 MHz for ^{13}C on a Brucker Advance III spectrometer. For NMR spectra, deuterated chloroform ($CDCl_3$) or deuterated methanol (CD_3OD) was used as the solvent. The chemical shift (δ) in ppm; coupling

constants (J); relative intensity is indicated by the number of protons (H); multiplicities are indicated by singlet (s), doublet (d), double-doublet (dd), triplet (t), quadruple (q) and multiplet (m); coupling constants are given in Hertz (Hz).

3.2 Procedure for the preparation of compounds 3 to 9

3.2.1 Synthesis of 1-(7-(diethylamino)-4-methyl-2*H*-chromen-2-ylidene)-piperidin-1-ium nitrate (3). A mixture of compound **2** (200 mg, 0.809 mmol, 1.0 eq.), piperidine (120 μL, 1.21 mmol, 1.5 eq.) and silver nitrate (343 mg, 2.02 mmol, 2.5 eq.), in dry acetonitrile (10 mL) was stirred at room temperature for 2 hours. The reaction was continuously monitored by TLC, using $CHCl_3/CH_3OH/H_2O$ (65 : 10 : 1). The reaction product was isolated by flash chromatography, using $CHCl_3/CH_3OH$ (9 : 1) and $CHCl_3/CH_3OH$ (8 : 2) as eluents, to yield 1-(7-(diethylamino)-4-methyl-2*H*-chromen-2-ylidene)piperidin-1-ium nitrate (248 mg, 85%). ^{1}H NMR (400 MHz, $CDCl_3$): 1.24 (6H, t, J = 7.1 Hz, $N(CH_2CH_3)_2$), 1.80–1.82 (6H, m, H-15, H-16, H-17), 2.58 (3H, s, 4-CH_3), 3.47 (4H, q, J = 7.1 Hz, $N(CH_2CH_3)_2$), 3.94–4.01 (4H, m, H-14, H-18), 6.61 (1H, d, $J_{8,6}$ = 2.4 Hz, H-8), 6.78 (1H, dd, $J_{6,5}$ = 9.2 Hz, $J_{6,8}$ = 2.4 Hz, H-6), 6.95 (1H, s, H-3), 7.56 (1H, d, $J_{5,6}$ = 9.2 Hz, H-5). ^{13}C NMR (100 MHz, $CDCl_3$): 12.5 (C-11, C-13), 19.4 (C-9), 23.6 (C-16), 26.0 (C-15, C-17), 45.2 (C-10, C-12), 46.8 (C-14/C-18), 48.8 (C-14/C-18), 96.5 (C-8), 100.7 (C-3), 109.2 (C-4a), 111.8 (C-6), 127.0 (C-5), 158.4 (C-4), 152.6 (C-7), 154.2 (C-8a), 160.0 (C-2). FTMS(+) calc. for $C_{19}H_{27}N_2O[M–(NO_3^-)]^+$ 299.2117 found 299.2111. UV λ_{max} (nm, CH_3CN): 261, 298, 437. ε (cm^{-1} M^{-1}): 21 000. Φ_F = 0.14.

3.2.2 Synthesis of (*E*)-1-(7-(diethylamino)-4-(4-(methoxycarbonyl)styryl)-2*H*-chromen-2-ylidene)piperidin-1-ium nitrate (4). A mixture of compound **3** (154 mg, 0.426 mmol, 1.0 eq.), methyl 4-formylbenzoate (26 mg, 0.426 mmol, 1.0 eq.) and piperidine (42 μL, 0.426 mmol, 1.0 eq.), in dry acetonitrile (25 mL), was stirred at 85 °C for 6 hours. The reaction was continuously monitored by tlc, using $CHCl_3/CH_3OH$ (9 : 1) as the eluent. The reaction product was isolate by flash chromatography, using $CHCl_3$ and $CHCl_3/CH_3OH$ (8 : 2) as eluents, to yield (*E*)-1-(7-(diethylamino)-4-(4-(methoxycarbonyl)styryl)-2*H*-chromen-2-ylidene)piperi-din-1-ium nitrate (130 mg, 60%). ^{1}H NMR (400 MHz, $CDCl_3$): 1.26 (6H, t, J = 7.2 Hz, $N(CH_2CH_3)_2$), 1.80–1.89 (6H, m, H-15, H-16, H-17), 3.49 (4H, q, J = 7.2 Hz, $N(CH_2CH_3)_2$), 3.90 (3H, s, CH_3), 3.96–4.21 (4H, m, H-14, H-18), 6.53 (1H, d, $J_{8,6}$ = 2.4 Hz, H-8), 6.84 (1H, dd, $J_{6,5}$ = 9.2 Hz, $J_{6,8}$ = 2.4 Hz, H-6), 7.49 (1H, d, $J_{19,9}$ = 16 Hz, H-19), 7.52 (1H, s, H-3), 7.83 (2H, d, $J_{21,22}$ = 8.4 Hz, H-21, H-25), 7.89 (1H, d, $J_{5,6}$ = 9.2 Hz, H-5), 7.95 (2H, d, $J_{22,21}$ = 8.4 Hz, H-22, H-24), 8.37 (1H, d, $J_{9,19}$ = 16 Hz, H-9).^{13}C NMR (100 MHz, $CDCl_3$): 12.6 (C-11, C-13), 23.8 (C-16), 26.2 (C-15, C-17), 45.2 (C-10, C-12), 46.8 (C-14/C-18), 49.2 (C-14/C-18), 52.3 (OCH_3), 95.2 (C-3), 96.8 (C-8), 108.0 (C-4a), 112.0 (C-6), 120.8 (C-19), 127.0 (C-5), 128.6 (C-21, C-25), 129.9 (C-22, C-24), 130.8 (C-23), 140.1 (C-4), 141.6 (C-9), 152.5 (C-7, C-20), 154.6 (C-8a), 160.0 (C-2), 166.7 (C-27). FTMS(+) calc. for $C_{28}H_{33}O_3N_2[M–(NO_3^-)]^+$ 445.24857 found 445.2479. UV λ_{max} (nm, CH_3CN): 362, 484. ε (cm^{-1} M^{-1}): 18 000. Φ_F = 0.08.

3.2.3 Synthesis of (*E*)-1-(7-(diethylamino)-4-styryl-2*H*-chromen-2-ylidene)-piperidin-1-ium nitrate (5). A mixture of compound **3** (276 mg, 0.764 mmol, 1.0 eq.), benzaldehyde (93 μL, 0.764 mmol, 1.0 eq.) and piperidine (76 μL, 0.755 mmol, 1.0 eq.), in dry acetonitrile (10 mL) was stirred at 85 °C for 5 minutes. The reaction was continuously monitored by tlc, using CH_2Cl_2/hexane (8 : 2) as the eluent. The reaction product was isolated by flash chromatography, using CH_2Cl_2/hexane (8 : 2) as eluent, to yield (*E*)-1-(7-(diethylamino)-4-styryl-2*H*-chromen-2-ylidene)piperidin-1-ium nitrate (309 mg, 90%). ^{1}H NMR (400 MHz, $CDCl_3$): 1.24 (6H, t, J = 7.2, $N(CH_2CH_3)_2$), 1.73–1.79 (6H, m, H-15, H-16, H-17), 3.46 (4H, q, J = 7.1 Hz, $N(CH_2CH_3)_2$), 3.91–3.97 (4H, m, H-14, H-18), 6.57 (1H, d, $J_{8,6}$ = 2.4 Hz, H-8), 6.81 (1H, dd, $J_{6,5}$ = 9.2 Hz, $J_{6,8}$ = 2.4, H-6), 7.18 (1H, s, H-3), 7.30–7.33 (3H, m, H-22, H-23, H-24), 7.35 (1H, d, $J_{9,19}$ = 16 Hz, H-9), 7.68 (2H, dd, $J_{21,22}$ = 8.0 Hz, $J_{21,23}$ = 2.0 Hz, H-21, H-25), 7.81 (1H, d, $J_{5,6}$ = 9.2 Hz, H-5), 8.01 (1H, d, $J_{19,9}$ = 16 Hz, H-19). ^{13}C NMR (100 MHz, $CDCl_3$): 12.6 (C-11, C-13), 23.7 (C-16), 26.1 (C-15, C-17), 45.2 (C-10, C-12), 46.8 (C-14/C-18), 48.7 (C-14/C-18), 93.9 (C-3), 97.0 (C-8), 107.8 (C-4a), 111.9 (C-6), 118.5 (C-9), 126.7 (C-5), 128.6 (C-21, C-25), 128.9 (C-22, C-24), 130.2 (C-23), 135.6 (C-20), 142.5 (C-19), 152.5 (C-7), 152.9 (C-4), 154.6 (C-8a), 159.9 (C-2). FTMS(+) calc. for $C_{26}H_{31}N_2O[M–(NO_3^-)]^+$ 387.2431 found 387.2424. UV λ_{max} (nm, CH_3CN): 282, 301, 467. ε (cm^{-1} M^{-1}): 17 000. Φ_F = 0.34.

3.2.4 Synthesis of (*E*)-1-(7-(diethylamino)-4-(4-(dimethylamino)styryl)-2*H*-chromen-2-ylidene)piperidin-1-ium nitrate (6). A mixture of compound **3** (162 mg, 0.448 mmol, 1.0 eq.), 4-(dimethylamino)benzaldehyde (67 mg, 0.448 mmol, 1.0 eq.) and piperidine (44 μL, 0.445 mmol, 1.0 eq.), in dry acetonitrile (10 mL) was stirred at 85 °C for 24 hours. The reaction was continuously monitored by tlc, using $CHCl_3$ as the eluent. The reaction product was isolated by flash chromatography, using CH_2Cl_2/hexane (8 : 2), CH_2Cl_2/hexane (9 : 1) and CH_2Cl_2 as eluents, to yield (*E*)-1-(7-(diethylamino)-4-(4-(dimethylamino) styryl)-2*H*-chromen-2-ylidene)piperidin-1-ium nitrate (205 mg, 92%). ^{1}H NMR (400 MHz, $CDCl_3$): 1.26 (6H, t, J = 7.2 Hz, $N(CH_2CH_3)_2$), 1.80–1.82 (6H, m, H-15, H-16, H-17), 3.04 (6H, s, 2× NCH_3), 3.49 (4H, q, J = 7.2 Hz $N(CH_2CH_3)_2$), 4.00 (4H, m, H-14, H-18), 6.59 (1H, d, $J_{8,6}$ = 2.4, H-8), 6.68 (2H, d, J = 8.8 Hz, H-22, H-24), 6.80 (1H, dd, $J_{6,5}$ = 8.8 Hz, $J_{6,8}$ = 2.4 Hz, H-6), 7.10 (1H, s, H-3), 7.18 (1H, d, $J_{9,17}$ = 15.8 Hz, H-9), 7.69 (1H, d, J = 8.8 Hz, H-21, H-25), 7.85 (1H, d, $J_{5,6}$ = 8.8 Hz, H-5), 8.11 (1H, d, $J_{19,9}$ = 15.8 Hz, H-19). ^{13}C NMR (100 MHz, $CDCl_3$): 12.7 (C-11, C-13), 23.9 (C-16), 26.2 (C-15, C-17), 40.3 (C-26, C-27), 45.2 (C-10, C-12), 47.5 (C-14/C-18), 48.4 (C-14/C-18), 91.5 (C-3), 97.0 (C-8), 108.2 (C-4a), 111.5 (C-6), 112.1 (C-22, C-24), 112.2 (C-9), 123.6 (C-20), 126.6 (C-5), 131.0 (C-21, C-25), 144.3 (C-19), 152.2 (C-7, C-23), 153.5 (C-4), 154.7 (C-8a), 159.8 (C-2). FTMS(+) calc. for $C_{28}H_{36}N_3O[M–(NO_3^-)]^+$ 430.2853 found 430.2845. UV λ_{max} (nm, CH_3CN): 282, 485. ε (cm^{-1} M^{-1}): 39 000. Φ_F = 0.98.

3.2.5 Synthesis of (*E*)-1-(7-(diethylamino)-4-(4-methoxystyryl)-2*H*-chromen-2-ylidene)piperidin-1-ium nitrate (7). A mixture of compound **3** (150 mg, 0.415 mmol, 1.0 eq.), 4-methoxybenzaldehyde (50 μL, 0.415 mmol, 1.0 eq.) and piperidine (41 μL, 0.415 mmol, 1.0 eq.) in dry acetonitrile (10 mL), was stirred at 85 °C for 18 hours. The reaction was continuously monitored by tlc, using $CHCl_3/CH_3OH/H_2O$ (65 : 20 : 2) as the eluent. The reaction product was isolated by flash chromatography, using $CHCl_3/CH_3OH/H_2O$ (65 : 20 : 2) as the eluent, to

yield (*E*)-1-(7-(diethylamino)-4-(4-methoxystyryl)-2*H*-chromen-2-ylidene)piperidin-1-ium nitrate (171 mg, 86%). ^{1}H NMR (400 MHz, $CDCl_3$): 1.24 (6H, t, J = 7.1, N(CH_2CH_3)$_2$), 1.75–1.80 (6H, m, H-15, H-16, H-17), 3.47 (4H, q, J = 7.1, N(CH_2CH_3)$_2$), 3.79 (3H, s, H-26), 3.97 (4H, m, H-14, H-18), 6.57 (1H, d, $J_{8,6}$ = 2.2 Hz, H-8), 6.79 (1H, dd, $J_{6,5}$ = 9.2 Hz, $J_{6,8}$ = 2.2 Hz, H-6), 6.85 (2H, d, $J_{22,21}$ = 8.6 Hz, H-22, H-24), 7.18 (1H, s, H-3), 7.24 (1H, d, $J_{9,19}$ = 15.9 Hz, H-9), 7.70 (1H, d, $J_{21,22}$ = 8.6 Hz, H-21, H-25), 7.84 (1H, d, $J_{5,6}$ = 9.2 Hz, H-5), 8.06 (1H, d, $J_{19,9}$ = 15.8 Hz, H-19). ^{13}C NMR (100 MHz, $CDCl_3$): 12.6 (C-11, C-13), 23.9 (C-16), 26.1 (C-15, C-17), 44.6 (C-14/C-18) 45.2 (C-10, C-12), 46.5 (C-14/C-18), 55.5 (C-26), 93.0 (C-3), 97.0 (C-8), 108.0 (C-4a), 111.7 (C-6), 114.4 (C-22, C-24), 115.8 (C-9), 126.7 (C-5), 128.5 (C-20), 131.6 (C-21, C-25), 142.7 (C-19), 152.4 (C-7), 153.2 (C-4), 154.7 (C-8a), 159.9 (C-2), 161.6 (C-23). FTMS(+) calc. for $C_{27}H_{33}O_2N_2$[M–(NO_3^-)]$^+$ 417.25365 found 417.2527. UV λ_{max} (nm, CH_3CN): 410. ε (cm^{-1} M^{-1}): 30 000. Φ_F = 0.82.

3.2.6 Synthesis of (*E*)-1-(4-(4-((5-carboxypentyl)oxy)styryl)-7-(diethylamino)-2*H*-chromen-2-ylidene)piperidin-1-ium nitrate (8). A mixture of compound **3** (232 mg, 0.642 mmol, 1.0 eq.), 6-(4-formylphenoxy) hexanoic acid (152 mg, 0.642 mmol, 1.0 eq.) and piperidine (63 μL, 0.642 mmol, 1.0 eq.) in dry acetonitrile (10 mL) was stirred at 85 °C for 5 h. The reaction was continuously monitored by tlc using $CHCl_3$/CH_3OH (9 : 1) as the eluent. The reaction product was isolated by flash chromatography, using $CHCl_3$/CH_3OH (95 : 5), $CHCl_3$/CH_3OH (9 : 1) and $CHCl_3$/CH_3OH (8 : 2) as eluents, to yield (*E*)-1-(4-(4-((5-carboxypentyl) oxy)styryl)-7-(diethylamino)-2*H*-chromen-2-ylidene)piperidin-1-ium nitrate (261 mg, 70%). ^{1}H NMR (400 MHz, CD_3OD): 1.26 (6H, t, J = 7.1 Hz, N(CH_2CH_3)$_2$), 1.53 (2H, m, H-28), 1.69 (2H, m, H-29), 1.78–1.83 (2H, m, H-27), 1.83 (6H, m, H-15, H-16, H-17), 2.32 (2H, t, H-30), 3.56 (4H, q, J = 7.1 Hz, N(CH_2CH_3)$_2$), 3.97 (4H, m, H-14, H-18), 4.02 (2H, t, H-26), 6.84 (1H, d, $J_{8,6}$ = 2.2 Hz, H-8), 6.95–6.98 (1H, dd, $J_{6,5}$ = 9.2 Hz, $J_{6,8}$ = 2.2 Hz, H-6), 6.98 (1H, s, H-3), 6.96 (2H, d, J = 8.4 Hz, H-22, H-24), 7.49 (1H, d, $J_{9,19}$ = 15.9 Hz, H-9), 7.70 (2H, d, J = 8.4 Hz, H-21, H-25), 7.83 (1H, d, $J_{19,9}$ = 15.9 Hz, H-19), 8.03 (1H, d, $J_{5,6}$ = 9.2 Hz, H-5). ^{13}C NMR (100 MHz, CD_3OD): 12.8 (C-11, C-13), 24.8 (C-16), 26.1 (C-29), 26.8 (C-28), 27.0 (C-15, C-17), 30.0 (C-27), 35.6 (C-30), 45.7 (C-14/C-18), 46.0 (C-10, C-12), 47.6 (C-14/C-18), 69.1 (C-26), 93.0 (C-3), 98.0 (C-8), 109.0 (C-4a), 113.0 (C-6), 116.1 (C-22, C-24), 117.5 (C-9), 127.9 (C-5), 129.6 (C-20), 131.3 (C-21, C-25), 142.5 (C-19), 154.1 (C-7), 154.7 (C-4), 156.3 (C-8a), 161.5.9 (C-2), 162.7 (C-23). FTMS(+) calc. for $C_{32}H_{41}O_4N_2$[M–(NO_3^-)]$^+$ 517.30608 found 517.3055. UV λ_{max} (nm, CH_3CN): 406, 478. ε (cm^{-1} M^{-1}): 30 000. Φ_F = 0.90.

3.2.7 Synthesis of (*E*)-1-(7-(diethylamino)-4-(4-((6-((2,5-dioxopyrrolidin-1-yl)oxy)-6-oxohexyl)oxy)styryl)-2*H*-chromen-2-ylidene)piperidin-1-ium nitrate (9). A mixture of compound **8** (160 mg, 0.309 mmol, 1.0 eq.), DCC (77 mg, 0.371 mmol, 1.2 eq.), DMAP (4 mg, 0.0309 mmol, 10%) in dry DMF (2 mL) and dry acetonitrile (25 mL) was stirred at room temperature for 5 minutes. After this period *N*-hydroxysuccinimide (43 mg, 0.371 mmol, 1.2 eq.) was added and the reaction mixture was stirred at room temperature for 6 h. The reaction was monitored by tlc, using $CHCl_3$/CH_3OH/H_2O (65 : 20 : 2) as the eluent. The reaction product was isolated by flash chromatography, using $CHCl_3$/CH_3OH (95 : 5), $CHCl_3$/CH_3OH (9 : 1) and $CHCl_3$/CH_3OH (8 : 2) as eluents, to yield (*E*)-1-(7-(diethylamino)-4-(4-((6-((2,5-dioxopyrrolidin-1-yl)oxy)-6-oxohex-yl)oxy)styryl)-2*H*-chromen-2-ylidene)piperidin-1-ium nitrate (200 mg, 98%). ^{1}H NMR (400 MHz, $CDCl_3$): 1.22 (6H, t, J = 7.1 Hz, N(CH_2CH_3)$_2$), 1.57 (2H, m, H-28), 1.72–1.82 (2H, m, H-15, H-16, H-17, H-27, H-29), 2.61 (2H, t, H-30), 2.82 (4H, s, H-33, H-34), 3.45 (4H, q, J = 7.1 Hz, N(CH_2CH_3)$_2$), 3.92 (4H, m, H-14, H-18), 3.93 (2H, t, H-26), 6.55 (1H, d, $J_{8,6}$ = 2.3 Hz, H-8), 6.79 (1H, dd, $J_{6,5}$ = 9.2 Hz, $J_{6,8}$ = 2.3 Hz, H-6), 6.82 (2H, d, J = 8.8 Hz, H-22, H-24), 7.07 (1H, s, H-3), 7.22 (1H, d, $J_{9,19}$ = 15.9 Hz, H-9), 7.64 (2H, d, J = 8.8 Hz, H-21, H-25), 8.82 (1H, d, $J_{5,6}$ = 9.2 Hz, H-5), 7.94 (1H, d, $J_{19,9}$ = 15.9 Hz, H-19). ^{13}C NMR (100 MHz, $CDCl_3$): 12.6 (C-11, C-13), 23.7 (C-16), 24.4 (C-29), 25.3 (C-28), 25.7 (C-33, C-34), 26.0 (C-15, C-17), 28.7 (C-27), 31.0 (C-30), 45.1 (C-10, C-12), 46.7 (C-14/C-18), 48.4 (C-14/C-18), 67.7 (C-26), 92.7 (C-3), 96.9 (C-8), 107.9 (C-4a), 111.8 (C-6), 115.0 (C-22, C-24), 115.7 (C-9), 126.7 (C-5), 128.3 (C-20), 130.5 (C-21, C-25), 142.5 (C-19), 152.4 (C-7), 153.1 (C-4), 154.6 (C-8a), 159.8 (C-2), 161.0 (C-23), 168.6 (C-31), 169.4 (C-32, C-35). FTMS(+) calc. for $C_{36}H_{44}O_6N_3$[M–(NO_3^-)]$^+$ 614.32 246 found 614.3215. UV λ_{max} (nm, CH_3CN): 404, 480. ε (cm^{-1} M^{-1}): 30 000. Φ_F = 0.92.

3.3 Quantum chemical calculations

All quantum chemical calculations were carried out with the Gaussian 16 software package.[39] The hybrid PBE0 functional[40] together with the standard 6-31G(d,p) basis set was used for geometry optimizations of both the ground and the first excited-states, without any symmetry constraints, while the larger 6-311+G(d,p) basis set was employed for the spectra calculations. Solvent effects were treated by means of the implicit polarized continuum model (PCM).[41,42] Frequency analysis was performed both in the ground and excited state, confirming the optimized structures as minima, presenting all frequencies real-valued.

4 Conclusions

In conclusion, with the objective to extend the delocalization of the π-electron system, we have designed and synthesized new 2-piperidinium-4-styrylcoumarin derivatives, with large Stokes shifts and high fluorescence quantum yields, using an efficient and low-cost synthetic strategy. From the results obtained from the UV/Vis spectra, it can be concluded that the 1-(7-(diethylamino)-4-methyl-2*H*-chromen-2-ylidene)piperidin-1-ium nitrate (**3**) is a useful intermediate in the synthesis of promising new fluorescent labels for biomolecules. The conducted DFT and TD-DFT calculations found significant geometric differences in the ground and excited states that helped to rationalize the emission process. The synthesis of other red-shifted coumarin fluorescent labels for biomolecules with improved features is currently in progress in our laboratory and the results will be reported briefly.

Author contributions

Conceptualization: R. E. and A. P.; investigation: R. E., J. P. R. and A. P.: supervision: A. P.; calculation: J. P. R.; writing –

original draft: R. E., J. P. R., A. T. C. and A. P.; writing – review & editing: A. P.

Conflicts of interest

There are no conflicts to declare.

Acknowledgements

The study was performed under the framework of THE SCREAM Project-"Touchstone for Heritage Endangered by Salt Crystallization, a Research Enterprise on the Art of Munch" (ref. FCT-ALT20-03-0145-FEDER-031577) financed by the Portuguese Foundation for Science and Technology (FCT) through National and European Funds, PROBIOMA project (0483_PROBIOMA_5_E, EP), co-financed by the FEDER, through the programme INTERREG VA España—Portugal (POCTEP) and the City University of Macau endowment to the Sustainable Heritage Chair.

Notes and references

1 M. V. Sednev, V. N. Belov and S. W. Hell, *Methods Appl. Fluoresc.*, 2015, **3**, 042004.
2 B. Giepmans, S. Adams, M. Ellisman and R. Tsien, *Science*, 2006, **312**, 217–224.
3 R. W. Dirks and H. J. Tanke, *BioTechniques*, 2006, **40**, 489–495.
4 M. Maekawa and G. D. Fairn, *J. Cell Sci.*, 2014, **127**, 4801–4812.
5 J. Chen, W. Liu, B. Zhou, G. Niu, H. Zhang, J. Wu, Y. Wang, W. Ju and P. Wang, *J. Org. Chem.*, 2013, **78**, 6121–6130.
6 G. Hanson and B. Hanson, *Comb. Chem. High Throughput Screening*, 2008, **11**, 505–513.
7 D. Maurel, L. Comps-Agrar, C. Brock, M. Rives, E. Bourrier, M. Ayoub, H. Bazin, N. Tinel, T. Durroux, L. Prézeau, E. Trinquet and J. Pin, *Nat. Methods*, 2008, **5**, 561–567.
8 J. Yin, P. Straight, S. McLoughlin, Z. Zhou, A. Lin, D. Golan, N. Kelleher, R. Kolter and C. Walsh, *Proc. Natl. Acad. Sci. U. S. A.*, 2005, **102**, 15815–15820.
9 H. Sahoo, *RSC Adv.*, 2012, **2**, 7017–7029.
10 T. Hermanson, *Bioconjugate Techniques*, London, Elsevier, 3rd edn, 2013.
11 A. Pereira, S. Martins and A. T. Caldeira, Coumarins as Fluorescent Labels of Biomolecules, in *Phytochemicals in Human Health*, IntechOpen Publications, London, UK, 2019, vol. 1.
12 X. Fang, Y. Zheng, Y. Duan, Y. Liu and W. Zhong, *Anal. Chem.*, 2019, **91**, 482–504.
13 I. Johnson and M. Spence, *Molecular Probes™ Handbook – A Guide to Fluorescent Probes and Labeling Technologies*, Life Technologies, Thermo Fischer Scientific, 11th edn, 2010.
14 H. Kobayashi, M. Ogawa, R. Alford, P. Choyke and Y. Urano, *Chem. Rev.*, 2009, **110**, 2620–2640.
15 T. B. Ren, W. Xu, W. Zhang, X. X. Zhang, Z. Y. Wang, Z. Xiang, L. Yuan and X. B. Zhang, *J. Am. Chem. Soc.*, 2018, **140**, 7716–7722.
16 H. Schill, S. Nizamov, F. Bottanelli, J. Bierwagen, V. N. Belov and S. W. Hell, *Chem.–Eur. J.*, 2013, **19**, 16556–16656.
17 Y. Fu and N. S. Finney, *RSC Adv.*, 2018, **8**, 29051–29061.
18 B. Czaplińska, M. Malarz, A. Mrozek-Wilczkiewicz, A. Slodek, M. Korzec and R. Musiol, *Molecules*, 2020, **25**, 2488–2507.
19 Z. Gao, Y. Hao, M. Zheng and Y. Chen, *RSC Adv.*, 2017, **7**, 7604–7609.
20 X. Liu, Z. Xu and J. M. Cole, *J. Phys. Chem. C*, 2013, **117**, 16584–16595.
21 K. P. Barot, S. V. Jain, L. Kremer, S. Singh and M. D. Ghate, *Med. Chem. Res.*, 2015, **24**, 2771–2798.
22 M. Riveiro, N. De Kimpe, A. Moglioni, R. Vázquez, F. Monczor, C. Shayo and C. Davio, *Curr. Med. Chem.*, 2010, **17**, 1325–1338.
23 M. Lee, C. Yen, W. Yang, H. Chen, C. Liao, C. Tsai and C. Chen, *Org. Lett.*, 2004, **6**, 1241–1244.
24 S. Martins, J. Avó, J. Lima, J. Nogueira, L. Andrade, A. Mendes and A. Pereira, *J. Photochem. Photobiol., A*, 2018, **353**, 564–569.
25 S. K. Lanke and N. Sekar, *J. Fluoresc.*, 2016, **26**, 949–962.
26 G. Zhang, H. Zheng, M. Guo, L. Du, G. Liu and P. Wang, *Appl. Surf. Sci.*, 2016, **367**, 167–173.
27 K. Wilze and A. Johnson, *Handbook of Detergents, Chemistry, Production and Application of Fluorescent Whitening Agents, Part F*, Boca Raton: Taylor & Francis, CRC Press, 2007.
28 E. Zaorska, M. Konop, R. Ostaszewski, D. Koszelewski and M. Ufnal, *Molecules*, 2018, **23**, 2241.
29 A. Gandioso, R. Bresolí-Obach, A. Nin-Hill, M. Bosch, M. Palau, A. Galindo, S. Contreras, A. Rovira, C. Rovira, S. Nonell and V. Marchán, *J. Org. Chem.*, 2018, **83**, 1185–1195.
30 M. Bojtár, A. Kormos, K. Kis-Petik, M. Kellermayer and P. Kele, *Org. Lett.*, 2019, **21**, 9410–9414.
31 S. Martins, P. Branco and A. Pereira, *J. Braz. Chem. Soc.*, 2012, **23**, 688–693.
32 J. Gordo, J. Avó, J. Parola, J. Lima, A. Pereira and P. Branco, *Org. Lett.*, 2011, **13**, 5112–5115.
33 A. Gandioso, S. Contreras, I. Melnyk, J. Oliva, S. Nonell, D. Velasco, J. Garcia-Amorós and V. Marchán, *J. Org. Chem.*, 2017, **82**, 5398–5408.
34 D. Cao, Z. Liu, P. Verwilst, S. Koo, P. Jangjili, J. S. Kim and W. Lin, *Chem. Rev.*, 2019, **119**, 10403–10519.
35 Y. Xiao and X. Qian, *Coord. Chem. Rev.*, 2020, **423**, 213513.
36 L. Cisse, A. Djande, M. Capo-Chichi, A. Khonté, J. P. Bakhoum, F. Delattre, J. Yoda, A. Saba, A. Tine and J. J. Aaron, *J. Phys. Org. Chem.*, 2019, **33**, e4014.
37 Y. Chen, J. Zhao, H. Guo and L. Xie, *J. Org. Chem.*, 2012, **77**, 2192–2206.
38 J. Ma, Y. Zhang, H. Zhang and X. He, *RSC Adv.*, 2020, **10**, 35840–35847.
39 M. J. Frisch, G. W. Trucks, H. B. Schlegel, G. E. Scuseria, M. A. Robb, J. R. Cheeseman, G. Scalmani, V. Barone, G. A. Petersson, H. Nakatsuji, X. Li, M. Caricato, A. V. Marenich, J. Bloino, B. G. Janesko, R. Gomperts, B. Mennucci, H. P. Hratchian, J. V. Ortiz, A. F. Izmaylov, J. L. Sonnenberg, D. Williams-Young, F. Ding, F. Lipparini, F. Egidi, J. Goings, B. Peng, A. Petrone, T. Henderson,

D. Ranasinghe, V. G. Zakrzewski, J. Gao, N. Rega, G. Zheng, W. Liang, M. Hada, M. Ehara, K. Toyota, R. Fukuda, J. Hasegawa, M. Ishida, T. Nakajima, Y. Honda, O. Kitao, H. Nakai, T. Vreven, K. Throssell, J. A. Montgomery Jr, J. E. Peralta, F. Ogliaro, M. J. Bearpark, J. J. Heyd, E. N. Brothers, K. N. Kudin, V. N. Staroverov, T. A. Keith, R. Kobayashi, J. Normand, K. Raghavachari, A. P. Rendell, J. C. Burant, S. S. Iyengar, J. Tomasi, M. Cossi, J. M. Millam, M. Klene, C. Adamo, R. Cammi, J. W. Ochterski, R. L. Martin, K. Morokuma, O. Farkas, J. B. Foresman and D. J. Fox, *Gaussian 16, Revision B.01*, Gaussian, Inc., Wallingford CT, 2016.

40 C. Adamo and V. Barone, *J. Chem. Phys.*, 1999, **110**, 6158.

41 C. Amovilli, V. Barone, R. Cammi, E. Cancès, M. Cossi, B. Mennucci, C. S. Pomelli and J. Tomasi, *Adv. Quantum Chem.*, 1998, **32**, 227–261.

42 M. Cossi and V. Barone, *J. Chem. Phys.*, 2001, **115**, 4708.